POLITECNICO DI TORINO
Repository ISTITUZIONALE

Mass transport phenomena at the solid-liquid nanoscale interface in biomedical application

(Article begins on next page)

25 April 2024

MASS TRANSPORT PHENOMENA AT THE SOLID-LIQUID NANOSCALE INTERFACE IN BIOMEDICAL APPLICATION

ANNALISA CARDELLINI[*†], MATTEO FASANO[*], ELIODORO CHIAVAZZO[*] AND PIETRO ASINARI[*]

[*]Multi-scale-Modeling-Laboratory, Dipartimento di Energia (DENERG),
Politecnico di Torino,
Corso Duca degli Abruzzi 24, 10129 Torino, Italy
[*†]e-mail: annalisa.cardellini@polito.it, web site: http://www.polito.it/small

Key words: Nanomedicine, Nanoconfined Water, Water Transport Phenomena, Protein and Amino Acids, Molecular Dynamics.

Abstract. Understanding heat and mass transfer phenomena at solid-liquid nanoscale interface plays a crucial role for introducing novel and more rationally designed theranostic particles, drug with tailored features and for gaining new insight on the biomolecules functioning. For instance, the water transport properties in the proximity of Amyloid beta peptides can influence the formation of amyloid plaques found in the brains of Alzheimer patients.

In the present work, transport behavior of water molecules in nanoconfined conditions has been investigated. By means of equilibrium Molecular Dynamics (MD) simulations, characteristic length of water confinement has been evaluated in the proximity of several biomolecules such as proteins and amino acids. Moving from proteins to their building blocks (i.e. amino acids), a similarity in water behavior was initially expected; MD simulations results show, instead, a more complex picture revealing a difference between the potential of water nanoconfinement by either proteins or amino acids. Hence, the reduction of water mobility in the proximity of nanoscale interfaces does not rely only on the local physical and chemical properties of the biomolecules surface, but the effects of size and potentials overlap should be also taken into account.

1 INTRODUCTION

Nanomedicine is the science dealing with the design and development of therapeutic and/or diagnostic agents in the nanoscale range (i.e. diameters from 1 to 100 nm), including all the critical aspects linked to the transport and delivery of therapeutic molecules and drugs in the body. Several studies underline the importance of nanoscience in medicine. For instance, Nuclear Magnetic Resonance Imaging (NMRI), which is one of the most spread and powerful diagnostic techniques, is receiving great advantages thanks to the use of nanoparticles. Relaxivity parameters (r_1 and r_2) of MRI contrast agents are enhanced by nanoconfined conditions: for examples, Ananta et al. experimentally found r_1 increases by confining contrast agents in mesoporous silica [1], whereas, Gizzatov A. et al. proved similar results for r_2 of ultra small paramagnetic iron oxides nanoparticles (USPIOs) [2]. Other examples of successful coupling of nanotechnology to medicine come from therapeutic

application. Nanotechnology-based approaches to hyperthermia seem to have great potentiality and a reduced invasiveness [3][4].

In all the previous examples, the understanding of heat and mass transport phenomena at the nanoscale takes on great importance for designing patient-tailored and more performing biomedical devices. In particular, the modulation and precise control of the water molecules diffusion in the vicinity of MRI contrast agents allow remarkable improvement in imaging performance, whereas an accurate study of heat conduction in the proximity of heated nanoparticles can be extremily useful to design their shape, size and coating for thermal ablation. Moreover, also proteins may modify their structure and thus their functionality according to the dynamics of the surrounding water environment [5][6]. Enzymatic activity, molecular recognition and folding process of proteins are strongly influenced by surrounding water mobility [7][8]. Furthermore the hydration layer has a key role in the formation of protein aggregates, such as those involved in Alzheimer's and Parkinson's diseases [9][10].

The properties of water nanoconfinement and the reduced water mobility at the solid-liquid interfaces have been studied and scaled by Chiavazzo et al. [13][14]. After having evaluated the self-diffusion coefficient of water in several nanoconfined geometries, authors formulated a scaling behaviour for water molecules diffusion in confined configurations: $D(\theta) \cong D_B(1 - \theta)$ where D is the water self-diffusivity in the solvated system, D_B is the bulk self-diffusion coefficient of water and θ is a dimensionless parameter which is related to confinement conditions. In particular, θ is given by the ratio between the water confined volume and the total volume of water in the system.

In this article, the nanoconfinement of water has been studied in the proximity of proteins and their building blocks: amino acids. Numerous experimental and theoretical studies have already demonstrated that the water molecules in the proximity of a protein surface are subjected to confined dynamics [15][16]. Moreover several works have shown the important role of amino acids in the protein structure stabilization [26][27], or their influence on water viscosity [26]. However, a broad physical understanding of the water mobility modification in the vicinity of any protein is still a subject of investigation, mainly because of the variety of amino acids physicochemical properties (hydrophilic vs. hydrophobic).

Here, molecular dynamics simulations are used for evaluating the different water confining capabilities of a large variety of proteins and amino acids. The main results show the hydration layer around poroteins, forming beacause of the attractive potential with interface, is almost 40% bigger than the amino acids. The reason of this descrepacy has been attributed to the few atoms of proteins building blocks involving in the non-bonded interaction with water molecules. This latter evidence sheds light on the difficulty in diriving water confinement around proteins starting from their building blocks: just 20 amino acids can join with several possible configurations providing different proteins characteristics and functionality. Finally, some points of discussions for a future work are presented.

2 METHODOLOGY

2.1 Molecular Dynamics simulations

In order to study the water transport properties at the solid-liquid nanoscale interface, Molecular Dynamics (MD) simulations have been performed by GROMACS (GROningen

MAchine for Chimical Simulations) software [17]. By solving classical Newton's laws, MD simulations are able to describe the motions of single atoms within a complex molecule or particle.

In this study, equilibrium MD simulations have been carried out for five proteins (B1 Immunoglobulin binding-domain, 1PGB; Ubiquitin, 1UBQ; Green Fluorescence Protein, 1QXT; Lysozime, 1AKI; Leptine, 1AX8) and 13 amino acids. The proteins sample covers a large variety of these biomolecules, with different structure and functionality, which allows to deduce water confinement behavior independently from the specific protein characteristics. Among the 20 amino acids in nature, just some examples per each group (polar, charged and neutral) have been studied (Figure 1). Hence, hydrophobic as well as hydrophilic behavior is investigated. In detail we considered arginine (ARG), aspartic acid (ASP), glutamic acid (GLU) and lysine (LYS) as charged amino acids; asparagine (ASN), glutamine (GLN), serine (SER), threonine (THR) and tyrosine (TYR) among polar amino acids and valine (VAL), isoleucine (ISO), leucine (LEU) and glycine (GLY) for the neutral family.

The geometries of all the studied cases have been downloaded from the RCSP Protein Data Bank [18] and the topologies have been completed by including CHARMM27 [19][20] force field. Each of these biomolecules has been solvated in a dodecahedral box of water where solvent molecules are described by spc/e model [20]. Before minimizing the energy, ions are added where needed, in order to achieve the neutrality of the system. Then two equilibration steps of 100 ps each have been performed: the former has been computed within a canonical ensemble (fixed Number of particles, Volume and Temperature-NVT) at 300 K by imposing a V-Rescale thermostat [21] on both water and biomolecule; the latter (fixed Number of particles, Pressure and Temperature -NPT), equilibrates the system to 300 K and 1 bar pressure, by means of Parinello-Rahman barostat [23][24]. Finally a 1 ns simulation has been performed for the equilibrated system.

Confining characteristics of the considered biological surfaces are studied by post-processing MD trajectories at steady state conditions.
The solvent mobility has been described by the self-diffusion coefficient related to the slope of the mean square displacement (MSD) of water by the Einstein relation:

$$\lim_{t \to \infty} \langle \| \boldsymbol{r}_i(t) - \boldsymbol{r}_i(0) \|^2 \rangle_{i \in A} = 6Dt$$

where $\boldsymbol{r}_i(t)$ and $\boldsymbol{r}_i(0)$ are the position vectors of the solvent molecules at the time t, and at the time t = 0, respectively and D the self diffusion coefficient of water. The considered simulation time is larger compared to the typical time of the velocity autocorrelation function, so that any dynamical coherence of the molecules motion has disappeared. The GROMACs tool to compute the solvent self-diffusion is g_msd. Instead by g_sas, the solvent accessible surface (SAS) [25] of each bio-structure can be calculated. Both the total S_{tot} and local solvent accessible surface related to the single atom ($S_{loc,i}$) are readily computed by GROMACS, once the geometry of the system is known (e.g. in the form of a pdb file). Moreover, the g_sas option, "$-q$" provides a pdb file containing the Cartesian coordinates of the points forming the solvent accessible surface.
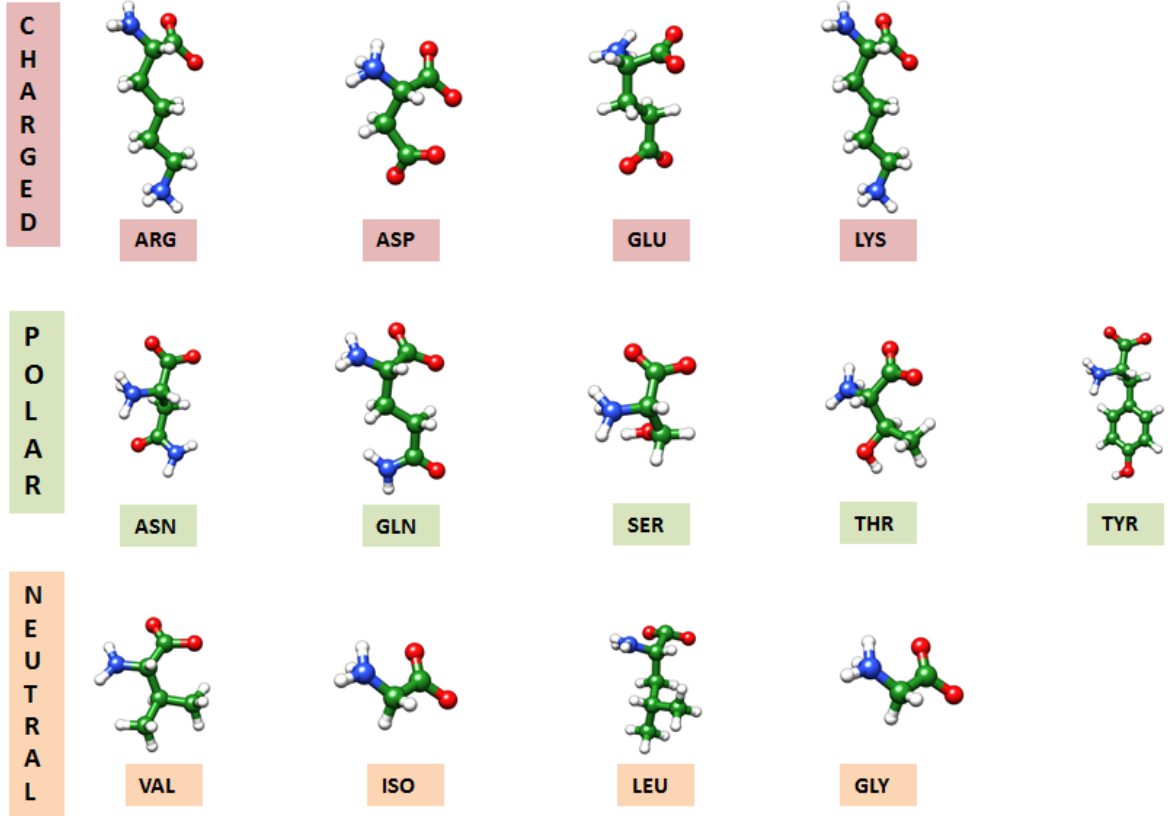
Figure 1: Structure of the 11 amino acids studied in the present work. Amino acids pictures are made with USCF Chimera [11].

2.2 Derivations of the characteristic length of water confinement

Moving from the bulk region to the proximity of solid-liquid surfaces, water molecules show a reduction of mobility and a more ordered structure. While in the bulk, fluid water molecules fluctuate with a kinetic energy proportional to $k_B T$, where k_B is the Boltzmann constant ($1.38 \times 10{-}23$ JK^{-1}) and T is the temperature, close to the solid surfaces they are subjected to Van der Waals (U_{vdw}) and Coulomb (U_c) interactions, which interfere with their state of agitation. This induces a layering of water molecules with reduced mobility at the soli-liquid interfaces, as already pointed out in other works [12].

Chiavazzo and colleagues [13] introduced a characteristic length, δ, to quantify the thickness of such confined water layer. The length δ is derived from the effective potential U_{eff} that water molecules feel at the Solvent Accessible Surfaces (SAS). The calculation takes into account just the interactions between water and the N atoms of the solid structure within a fixed cut-off radius (R_c), where R_c has been chosen large enough to include all atoms with a potential contribution different to zero, namely U_{eff} ~0. The corresponding effective potential energy U_{eff} is due to Van der Waals (U_{vdw}) and Coulomb (U_c) interactions and it has been computed as:

$$U_{eff}(n) = U_{vdw}(n) + \langle U_c \rangle(n), \tag{1}$$

4

where the *n*-axis is orthogonal to the SAS and it is passing through the center of the atom *i-th*. Van der Waals interactions are modelled by:

$$U_{vdw}(n) = \sum_{k=1}^{N_n} 4\varepsilon_k \left[\left(\frac{\sigma_k}{r_k} \right)^{12} - \left(\frac{\sigma_k}{r_k} \right)^6 \right], \tag{2}$$

with ε_k, σ_k and r_k denoting the depth of the potential well, the distance where such potential becomes zero (both obtained with Lorentz-Berthelot rule), and the Euclidean distance between the generic line point with coordinate *n* and the center of *k−th* nearest neighbour, respectively. For the Coulomb interactions, the average potential energy between the N atoms and the water dipoles, at a fixed temperature T, is

$$\langle U_C \rangle(n) = -E\mu_w \Gamma \left(\frac{E\mu_w}{k_B T} \right), \tag{3}$$

where E, μ_w, and Γ denote the electrical field strength, water dipole moment (7.50×10^{-30} C m for SPC/E model) and the Langevin function. The $\langle U_C \rangle(n)$ formulation is derived from the Maxwell-Boltzmann distribution of water dipoles orientation, due to the thermal agitation. Knowing the effective potential $U_{eff}(n)$ for the atom *i*, a corresponding characteristic length δ_i can be estimated. According to [13], δ_i is evaluated considering the depth within which the effective potential is stronger than water molecules thermal energy. Therefore, based on the definition of δ_i, all the water molecules located within such a distance are significantly affected by the Van der Waals and Coulomb interactions, whereas all the water molecules beyond the characteristic length δ_i can escape the potential well generated by the solid wall. In general, the quantity δ_i varies per each atom *i*. The mean characteristic length $\bar{\delta}$ of the overall solid surface can be derived as:

$$\bar{\delta} = \frac{\sum_{i=1}^{N} \delta_i S_{loc,i}}{S_{tot}}, \tag{4}$$

with $S_{loc,i}$ and N being the specific (per-atom) SAS for the atom *i* and the total number of atoms, respectively. Note that the above formulation is general and applies to hydrophilic and hydrophobic surfaces, regardless of their electrostatic surface charge.

3 RESULTS

3.1 Water confinement at solvent-proteins interfaces

The computed characteristic lengths of water confinement for the five proteins previously described are shown in Table 1. Although the study cases present strong differences in structure, shape and functionality, the thickness of water molecules layer forming in the proximity of proteins surfaces is comparable and it oscillates in the range: 0.305±0.01 nm. Hence, results show that independently from the specific protein, just few layers of water molecules are significantly affected by the effective potential of the solid surface.

Regarding the solvent accessible surface, values cover a range from 36.04 nm² (B1

Immunoglobulin binding-domain) to 108.8 nm^2 (Ubiquitin).

The self-diffusion coefficient of water in the proximity of the studied proteins is reduced respect to the bulk value ($2.6 \cdot 10^{-9}$ m^2/s [26]) and it goes from $2.364 \pm 0.025 \cdot 10^{-9}$ m^2/s (Lysozime protein) to $2.434 \pm 0.014 \cdot 10^{-9}$ m^2/s (B1 Immunoglobulin binding-domain protein). The latter results are in good agreement with the prediction of the scaling law suggested by [13].

Table 1: Mean characteristic length $\bar{\delta}$ of water nanoconfinement, solvent accessible surface (SAS) and water self-diffusion coefficient for five solvated proteins

Proteins	$\bar{\delta}$ [nm]	SAS [nm^2]	D [m^2/s]
1 PGB	0.295	36.04	$(2.434 \pm 0.014) \cdot 10^{-9}$
1UBQ	0.309	48.02	$(2.411 \pm 0.063) \cdot 10^{-9}$
1QXT	0.302	108.8	$(2.425 \pm 0.016) \cdot 10^{-9}$
1AKI	0.306	67.4	$(2.364 \pm 0.025) \cdot 10^{-9}$
1AX8	0.315	68.9	$(2.372 \pm 0.016) \cdot 10^{-9}$

3.2 Water confinement at solvent-amino acids interfaces

As described in the previous paragraph, the relation between water nanoconfinement length and proteins surface properties appears not so trivial: although proteins present different fuatures and configurations, they show the same ability in confining water at their surface. Because of this complexity a deeper investigation has been carried out on proteins building blocks: amino acids in dilute aqueous solution.

The combined use of molecular dynamics simulations and computational methods has brought to the results in Table 2. Although just slight differences are evident among the characteristic length of polar, charged and neutral amino acids, it is interesting to note that those with similar solvent accessible surface present values of $\bar{\delta}$ increasing with the hydrophilicity. For example, the water molecules layer in the proximity of aspartic acid ($\bar{\delta} = 0.18$ nm), is larger than the Valine characteristic length ($\bar{\delta} = 0.153$ nm). This result can be considered in line with the definition of δ: because of the presence of charged and polar residues in the side chain of aspartic acid, water molecules are affected by a deeper potential well and thus by a stronger confinement at the solid-liquid interface.

Concerning the self-diffusion coefficients of water in the proximity of the latter amino acids, D values are comparable to those of proteins.

Table 2: Mean characteristic length $\bar{\delta}$ of water nanoconfinement and solvent accessible surface (SAS) for the 13 amino acids considered

Charged amino acids	$\bar{\delta}$ [nm]	SAS [nm^2]
ARG	0.208	3.06
ASP	0.180	2.26
GLU	0.185	2.52
LYS	0.184	2.77

Polar amino acids	$\bar{\delta}$ [nm]	SAS [nm^2]
ASN	0.168	2.30
GLN	0.182	2.55
SER	0.163	1.98
THR	0.164	2.19
TYR	0.213	3
Neutral amino acids	$\bar{\delta}$ [nm]	SAS [nm^2]
VAL	0.153	2.29
ISO	0.167	2.51
LEU	0.180	2.57
GLY	0.155	1.65

3.3 Interpreting the mismatch between δ proteins and amino acids

A comparison between Table 1 and Table 2 clearly leads to the consideration that the mean characteristic length of confinement evaluated for the amino acids is almost 40% less than the proteins one. This mismatch becomes even more evident from the Figure 2 where, the average value of $\bar{\delta}$ is plotted for the three amino acids groups (charged, polar and neutral) and for the studied proteins.

It is well established that the hydration layer forming at the solvent-particle interface is strongly dependent on the surface physicochemical properties. However, since amino acids are proteins building blocks, the significant differences in terms of the mean characteristic length could result unclear. The latter behavior may be due to a size-dependent effect. In fact, because of the reduced number of atoms forming the amino acids, a water molecule in their proximity is subjected to a weak effective potential.

Two further analysis have been followed to prove the size dependent feature of δ. First, a MD configuration made out of two identical amino acids (arginine in this case) has been set-up (Figure 3a). The initial distance, h, between arginines centers of mass has been fixed at 3 nm and 1 ns equilibrium molecular dynamics simulation has been performed while fixing the amino acids relative position. In this case, each amino acid was characterized by its own $\bar{\delta}$, which exactly corresponds to the specific value reported in Table 2. Then, h was progressively decreased to 2 nm, 1nm up to 0.5 nm values (Figure 3b-d). As shown in Figure 3, the solvent accessible volume in the region between the amino acids (h) is reduced as the amino acids were forced to approach each other. At one extreme, when h = 0.5 nm, water molecules are no more able to wet the entire surface of the two arginines, but they can just access to the external part of the coupled molecules. Comparing the $\bar{\delta}$, obtained for each set-up, it is interesting to note an increase of the characteristic length of water confinement as the inter amino acids distance reduces (Table 3). This behavior is strictly connected to the effective potential overlap: as the arginines approach, more atoms are located within the cut-off radius, R_c, and thus more intense non-bonded interactions can be established between water molecules and the atoms of the bio-structure. Similar analysis has been repeated increasing the number of amino acids within the water box. Configurations with four and nine

amino acids are then simulated. As evident from Table 3, the mean characteristic length of water confinement further increases, as the amino acids distance reduces. A maximum value of 0.279 nm is reached in case of 9 arginine amino acids arranged in a 3x3 matrix with inter distances of 0.5 nm.
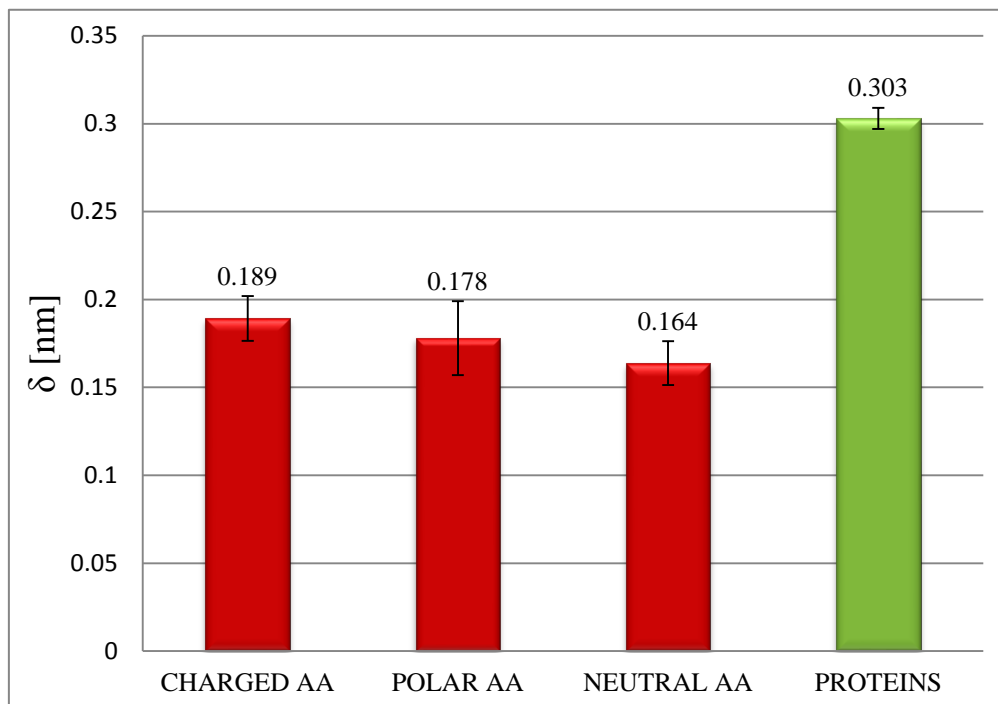

Figure 2: Comparison between amino acids' and protein' s characteristic length of water confinement. An avarage value of $\bar{\delta}$ is calculated among proteins and charged, polar, and neutral amino acids.

The latter value can be almost compared with the proteins hydration layer previously obtained, even if, probably the strong dipole of the peptide bonds (covalent chemical bonds formed when the amino group of one amino acid joins to the carboxyl group of its neighbor) can increase the effect of water confinement around a protein. Hence, in addition to the physicochemical properties of the solid surface, the water nanconfinement length is also influenced by the size of the considered molecule, and the potential overlapping assumes a relevant role to reduce the mobility of the polar solvent molecules close to the interfaces.

To confirm the argument of potential overlapping, a second analysis has been considered. The MD trajectories of the solvated Ubiquitin protein (1UBQ) have been performed. Then, just a small portion of 1UBQ solvent accessible surface was analyzed and the effective potential U_{eff} evaluated (Figure 4). Results in Figure 4 clearly show that the solvent felt the potential from several amino acids present in its vicinity. Hence, the water local confinement can be attributed to the complex overlapping of the non-bonded potentials arising from contiguous amino acids.

Table 3: Mean characteristic length $\bar{\delta}$ of water nanoconfinement and SAS for different configuration of coupled arginine amino acids.

n° Arginine molecules	h [nm]	$\bar{\delta}$ [nm]	SAS [nm^2]
1		0.208	3.06
2	3	0.198	6.21
2	2	0.209	6.23
2	1	0.216	6.09
2	0.5	0.255	5.11
4	0.5	0.256	9.10
9	0.5	0.279	16.15
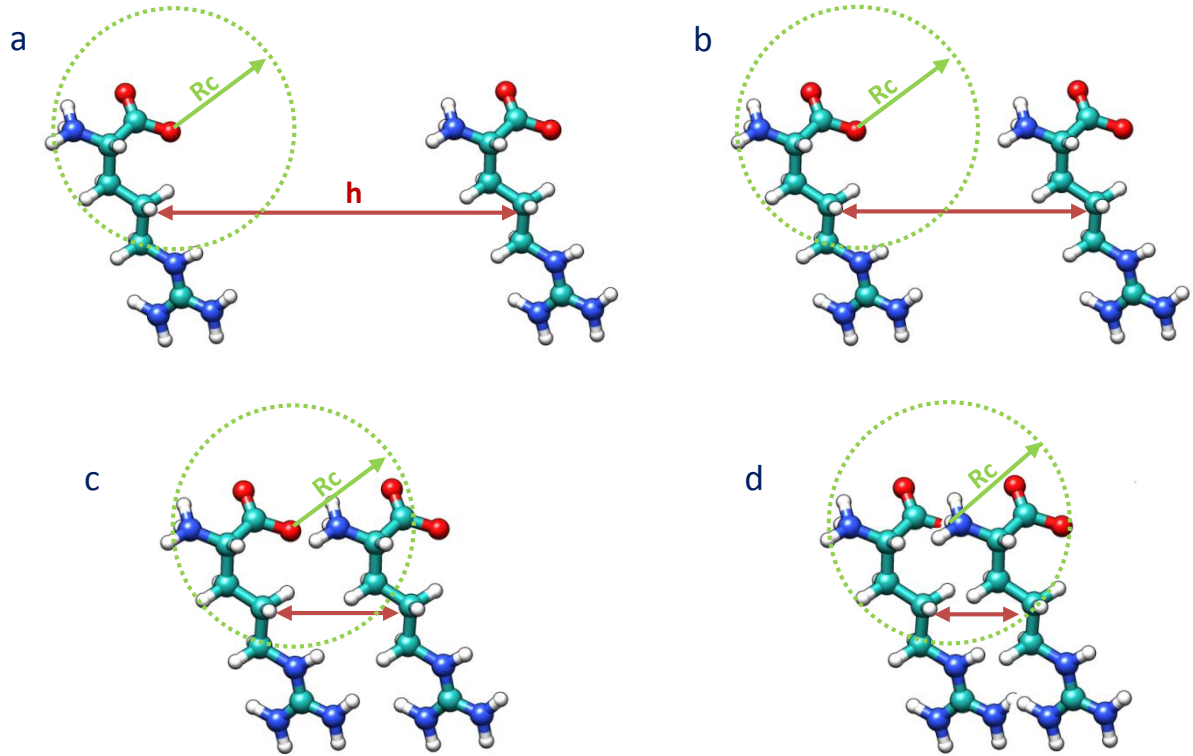
Figure 3: Two ARG amino acids at different distane h. a) h = 3nm b) h = 2nm. c) h = 1 nm. d) h = 0.5 nm. Atoms within the cut-off radius contribuite to the effective potential which influences the water mobility at the solid-liquid interfaces.
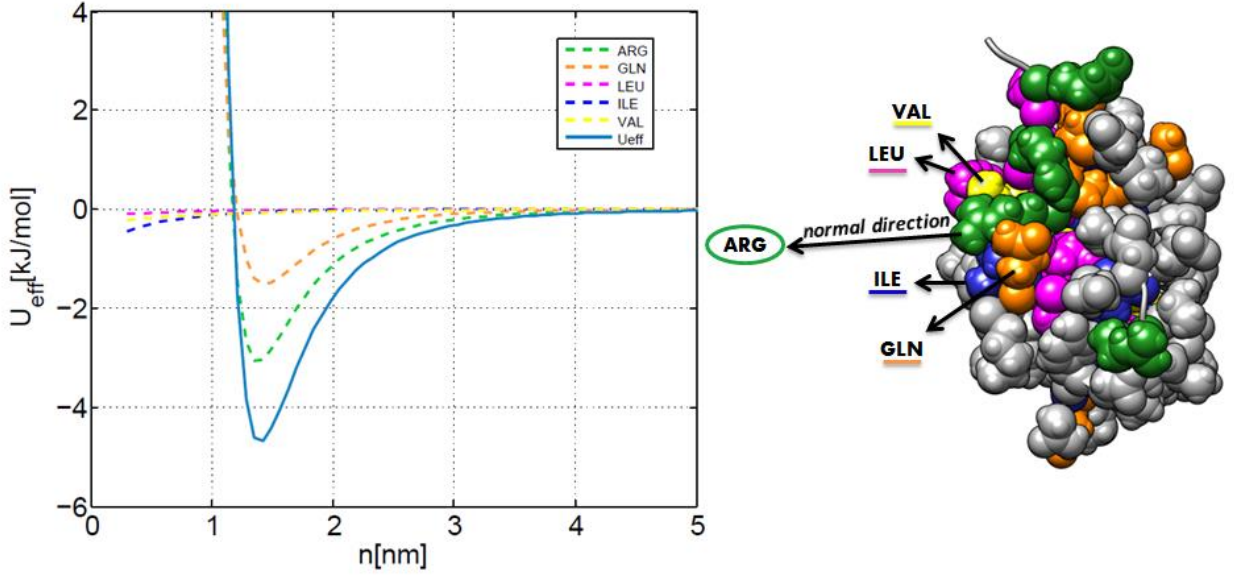
Figure 4: Local effective potential (U_{eff}) felt by water molecules located along one of the normal directions to Ubiquitin surface. Because of the precise position on the protein, the dominant contribution to the effective potential comes from arginine -ARG- and glutamic acid -GLN- atoms

4 CONCLUSIONS

The study of water dynamics under nanoconfined conditions has strong implication in nanomedicine, from the diagnostic to the therapeutic field.

In this work, the water transport behavior in the proximity of proteins and their building blocks, amino acids, has been investigated. By means of molecular dynamics simulations and matlab computational tools, the water confinement length $\bar{\delta}$ has been evaluated at some proteins and amino acids interface. The latter physical quantity is defined as the distance between a water molecule and the solid surface where the attractive non-bonded interactions of the solid prevail on the kinetic energy of the liquid, thus causing a reduced mobility for water. The analysis of several study cases has shown a consistent mismatch: the almost constant values of δ among different proteins ($\cong 0.3\ nm$) is significantly larger than the average one for amino acids ($\cong 0.19\ nm$). We have demonstrated that the hydration layer at the solid-liquid interface has a strong dependence on the biomolecules size, in addition to the physicochemical properties of the solid surface. Thus, the limited amount of atoms in the amino acids structure determines a weak attractive potential with the water molecules in their proximity and thus a reduced confinement length.

The latter evidence has been further proved by analyzing the $\bar{\delta}$ value in the light of the possible superposition principle of the solid-liquid non bonded potential. On one hand, $\bar{\delta}$ has been evaluated at the interface of two coupled amino acids at a variable distance, namely $h = 0.5 \div 3\ nm$. Moreover, also configurations with four and nine amino acids have been considered. On the other hand, the effective potential between water molecules and amino acids atoms has been calculated on a local portion of Ubiquitin surface. Results show that the enhanced water confinement capabilities of proteins do not depend on the average value of the amino acids one, but a cross interaction of the effective potential could occur. Therefore,

overall water confining properties of proteins are not strictly coupled to the ones of their building blocks, but they are enhanced by complex amino acids-amino acids interactions.

The study of the hydration layer around amino acids or very small peptides such as Alzheimer's amyloid-β(1–40) peptide could have implication in understaing the biomolecules aggragation, dynamics and functionality [29][30].

REFERENCES

[1] Ananta, J., Godin, B., Sethi, R., Moriggi, L., Liu, X., Serda, R.E., Krishnamurthy, R., Muthupillai, R., Bolskar, R.D., Helm, L., Ferrari, M., Wilson, L.J and Decuzzi, P. Geometrical confinement of gadolinium-based contrast agents in nanoporous particles enhances T1 contrast. *Nat. Nanotech.* (2010) **5**: 815.

[2] Gizzatov, A., Key, J., Aryal, S., Ananta, J., Cervadoro, A., Palange, A.L., Fasano, M., Stigliano, C., Zhong, M., Di Mascolo, D., Guven, A., Chiavazzo, E., Asinari, P., Liu, X., Ferrari, M., Wilson, L.J. and Decuzzi, P. Hierarchically structured magnetic nanoconstructs with enhanced relaxivity and cooperative tumor accumulation. *Adv. Funct. Mat.* (2014) **24**: 4584.

[3] Coss, R. and Linnemans W. The effects of hyperthermia of the cytoskeleton: a review. *International Journal of Hyperthermia* (1996) **12(2)**:173-196.

[4] Hildebraandt, B., Wust, P., Ahlers, O., Dieing, A., Sreenivasa, G., Kerner, T., Felix, R. and Riess, H. The cellular and molecular basis of hyperthermia. *Critical review in oncology/hematology* (2002) **43(1)**: 33-56.

[5] Zhou, H.-X. Macromolecular crowding and confinement: biochemical, biophysical, and potential physiological Consequences. *Annual review of biophysics* (2008) **37**:375.

[6] Ellis, R.J. and Minton, A.P. Cell biology: join the crowd. *Nature* (2003) **425(6953)**:27-28.

[7] Bizzarri, A.R. and Cannistraro, S. Molecular dynamics of water at the protein-solvent interface. *The Journal of Physical Chemistry B* (2002) **106(26)**:6617-6633.

[8] Best, R.B. and Hummer, G. Diffusive Model of proteins folding dynamics with Kramers turnover in rate. *Phys.Rev.Lett.* (2006) **96**:228104.

[9] Fernandez, A. and Scheraga, H.A. *Proc. Natl. Acad. Sci.* (2003) **100**:2391– 2396.

[10] Buchete, N.V. and Hummer, G. Structure and dynamics of parallel β-sheets, hydrophobic core and loops in Alzheimer's Aβ fibrils. *Biophys.J.* (2007) **92(9)**:3032-3039.

[11] Pettersen, E.F., Goddard, T.D., Huang, C.C., Couch, G.S., Greenblatt, D.M., Meng, E.C. and Ferrin, T.E. Ucsf chimera-a visualization system for exploratory research and analysis. *Journal of Computational Chemistry* (2004) **25(13)**:1605–1612.

[12] Castrillón, S.R.V., Giovambattista, N., Aksay, I. and Debenedetti, P.G. Effect of surface polarity on the structure and dynamics of water in nanoscale confinement. *J.Phys.Chem. B* (2009) **113**:1438-1446.

[13] Chiavazzo, E., Fasano, M., Asinari, P. and Decuzzi, P. Scaling behaviour for the water transport in nanoconfined geometry. *Nature Communications* (2014) **5**:4565.

[14] Fasano, M., Chiavazzo, E. and Asinari, P. Water transport control in carbon nanotube arrays. *Nanoscale Research letters* (2014) **9**:559.

[15] Denisov, V.P. and Halle, B. Protein hydration dynamics in aqueous solution. *Faraday Discussions* (1996) **103(0)**: 227–244.

[16] Tarek, M. and Tobias, D.J. The dynamics of protein hydration water: a quantitative comparison of molecular dynamics simulations and neutron-scattering experiments. *Biophysical journal* (2000) **79(6)**:3244–3257.

[17] Hess, B., Kutzner, C., Van der Spoel, D. and Lindahl, E. *J. Chem. Theory Comput.* (2008) **4**:435-447.

[18] www.rcsb.org

[19] MacKerell, AD.Jr, Feig, M. and Brooks, C.L. 3rd. Extending the treatment of backbone energetics in protein force fields: limitations of gas-phase quantum mechanics in reproducing protein conformational distributions in molecular dynamics simulations. *J. Comp. Chem*. (2004) **25(11)**:1400–15.

[20] MacKerell et al., All-atom empirical potential for molecular modeling and dynamics studies of proteins. *J. Phys. Chem. B*. (1998) **102(18)**:3586–3616.

[21] Berendsen, H.J.C., Grigera, J.R. and Strrtsma, T.P. The missing term in effective pair potentials. *J. Phys. Chem.* (1987) **91**:6269–6271.

[22] Bussi, G., Donadio, D. and Parrinello, M. *The Journal of Chemical Physics* (2007) **126**:014101.

[23] Parrinello, M. and Rahman, A. Polymorphic transitions in single crystals: A new molecular dynamics method. *J. Appl. Phys*. (1981) **52**:7182–7190.

[24] Nose, S. and Klein, M. L. Constant pressure molecular dynamics for molecular systems. *Mol. Phys*. (1983) **50**:1055–1076.

[25] Eisenhaber, F., Argos, P., Sander, C. and Scharf, M. *Comput. Chem*. (1995) **16**:273-284.

[26] Zhao, H. *Biophys. Chem.* (2006) **122**:157–183.

[27] Sterpone, F., Stirnemann, G., Hynes, J.T. and Laage, D. Water hydrogen-bond dynamics around amino acids: the key role of hydrophilic hydrogen-bond acceptor groups. (2010) **114**:2083-2089.

[28] Van der Spoel, D., van Maaren, P. J. and Berendsen, H. J. A systematic study of water models for molecular simulation: derivation of water models optimized for use with a reaction field. *J. Chem. Phys*. (1998) **108**:10220.

[29] Massi, F. and Straub, J.E. Structural and dynamical analysis of the hydration of the Alzheimer's beta-amyloid peptide. *J.Comput. Chem.* (2003) **24(2)**:143-53.

[30] Buchete, N.V., Tycko, R. and Hummer, G. Molecular dynamics simulations of Alzheimer's β-amyloid protofilaments. *J.Mol.Biol*. (2005) **363**:804-821.